IEEE Photonics Journal
An IEEE Photonics Society Publication

Open Access

Fourier and Inverse Fourier Transform Model for Delayed Self-interferometry System

Volume 12, Number 3, June 2020

Ling Zhang
Weilin Xie
Yuxiang Feng
Zhangweiyi Liu
Haijun Zhou
Yinxia Meng
Yuanshuo Bai
Wei Wei
Yi Dong

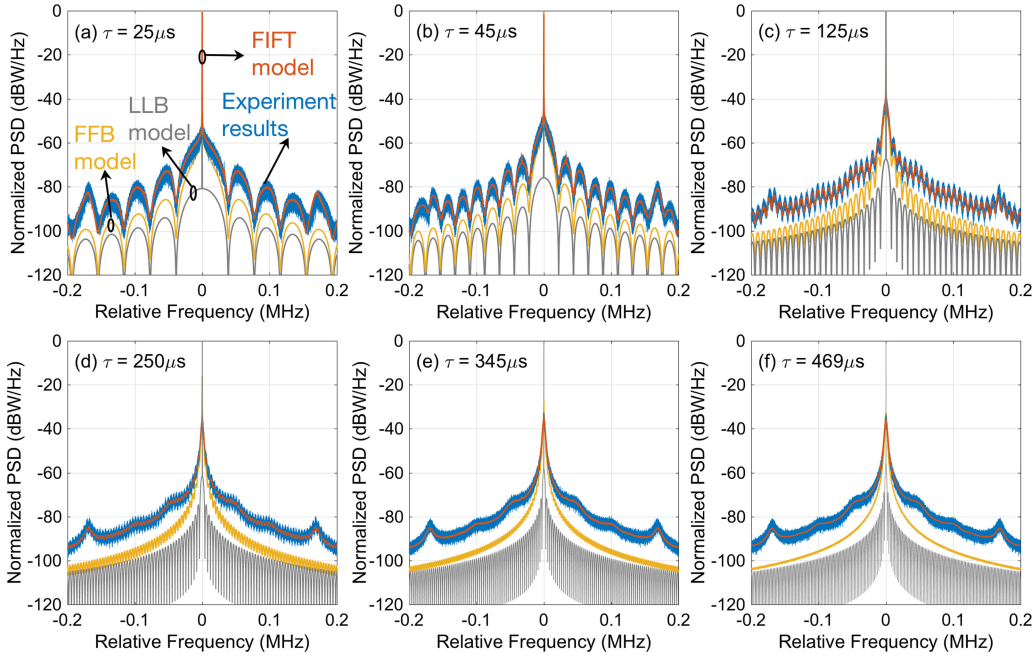

DOI: 10.1109/JPHOT.2020.2997248

Fourier and Inverse Fourier Transform Model for Delayed Self-interferometry System

Ling Zhang,[1] **Weilin Xie**,[2] **Yuxiang Feng**,[2] **Zhangweiyi Liu**,[1] **Haijun Zhou**,[1] **Yinxia Meng**,[2] **Yuanshuo Bai**,[1] **Wei Wei**,[2] **and Yi Dong** [2]

[1]State Key Laboratory of Advanced Optical Communication Systems and Networks, Shanghai Jiao Tong University, Shanghai 200240, China
[2]Key Laboratory of Photonics Information Technology, Ministry of Industry and Information Technology, School of Optics and Photonics, Beijing Institute of Technology, Beijing 100081, China

DOI:10.1109/JPHOT.2020.2997248

Manuscript received April 20, 2020; revised May 16, 2020; accepted May 19, 2020. Date of publication May 25, 2020; date of current version June 22, 2020. This work was supported in part by the National Natural Science Foundation of China under Grants 61805014, 61827807, and 61690193 and in part by China Postdoctoral Science Foundation under Grants 2018M630082, 2019T120051. Corresponding author: Weilin Xie. (e-mail: wlxie@bit.edu.cn).

Abstract: Understanding the effects of laser phase and frequency noise on laser interferometry is significant for evaluating the system performance. To precisely study the performance limit caused by laser frequency noise, here we propose and demonstrate a versatile model based on the Fourier and inverse Fourier transform (FIFT) method. This model, capable of estimating the beat note spectra of different delayed self-interferometry (DSI) with laser sources of arbitrary frequency noise properties, allows for accurate evaluations of the noise performance in a variety of interferometry based systems. Such a model has been experimentally validated using lasers with irregular frequency noise properties such as cavity stabilized fiber laser or laser under optical phase-locking, providing more detailed insight into the evolution of the frequency noise dynamics at different interferometric conditions. With average estimation goodness (AEG) of 0.9716 and computation complexity of $\mathcal{O}(N\log N)$, this model offers greater accuracy and lower complexity than conventional methods. It has also been confirmed that this model permits to distinguish the contributions from the laser frequency stability and other noise sources, which could be helpful for the noise analysis and performance optimization of the system.

Index Terms: Optical interferometry, laser frequency noise, optoelectronic phase-locked loop.

1. Introduction

Coherent laser interferometry in the form of delayed self-interferometry (DSI) is one of the most important fundamentals in a wide range of laser-based communication, measurement, and signal processing systems such as coherent optical communication [1], [2], coherent metrology [3]–[5], optical sensing [6]–[8], coherent optical interferometry and reflectometry [9], [10], and so on. The laser noise properties, especially in terms of spectral purity and frequency stability, are key factors that determine the performance of these systems [11]–[13]. It is thus of particular interest and significance to precisely describe the relationships between the system performance and laser

frequency noise characteristics. To this end, different models based on frequency domain analysis have been proposed.

Generally, conventional laser linewidth based (LLB) model is applied to assess the influence of laser frequency noise [14], [15]. Formulas of the beat signal autocorrelation function (ACF) and DSI spectrum have been presented. In this approach, laser linewidth is modeled to account for the contribution only from the white frequency noise. To take into account the nonnegligible contributions from other non-white frequency noise components such as flicker frequency noise [16] and random-walk frequency noise [17], frequency noise spectrum (FNS) fitting based (FFB) models have been developed [18]–[20]. As FNS contains all the possible noise components, it permits a more accurate description of the laser noise properties. For the noise components that have analytic solutions, the beat signal ACF or DSI spectrum can be calculated using the noise coefficients respectively. Usually, the coefficients are obtained by the proper fitting of FNS. This way, the whole DSI spectrum can be constructed with the convolution of the spectra arising from these analytically-resolved noise components. However, the fitting process and the convolution method bring complexity and massive calculation.

Nevertheless, in order to further improve the accuracy in predicting the DSI performance, the contributions from the non-analytically-resolved noise components [19] such as high-order $1/f^{\alpha}$ noise, pseudo-white noise caused by spontaneous emission, and pumping noise should also be accounted for. Besides, from a practical point of view, for lasers with irregular FNS such as spurs or glitches and servo-induced anomalous spectrum that are analytically-intractable, the aforementioned conventional approaches may encounter difficulties in the estimation and analysis.

In this work, we propose a more precise and efficient analysis model based on the Fourier and Inverse Fourier Transform (FIFT) method to study the impact of laser frequency noise on the DSI system. Without fitting or any approximation, the proposed model offers an accurate prediction for the DSI spectra at different interferometric conditions based on arbitrary laser frequency noise properties. Theoretical validations and the application-oriented experiments in practical environments are both investigated and discussed. Section 2.1 presents the theoretical description of the FIFT model. Numerical verification and comparison conducted in Section 2.2 prove that this model provides effectiveness and lower computation complexity $\mathcal{O}(N\log N)$ compared with conventional models ($\mathcal{O}(N^2)$). Then, as described in Section 3, practical demonstrations for model validation with experimental data have been carried out. Comparative experiments with cavity-stabilized fiber laser source in Section 4.1 show that the FIFT model offers higher accuracy with average estimation goodness (AEG) of 0.9716 than conventional models ($<$0.3155). Experiments in Sections 4.2 and 4.3 prove that for lasers with irregular frequency noise properties or an optoelectronic phase-locked loop (OPLL), the conventional models fail while the FIFT model still provides accurate estimates. As discussed in Section 5, the proposed model finds applications in identifying the noise sources in DSI systems, for instance, distinguishing the influence of laser intrinsic frequency noise and other noise sources such as the environment perturbations.

2. Principle

2.1 FIFT Model Description

The electrical field of a single-mode laser can be modeled as a quasi-monochromatic field $E(t) = E_0 \exp[j2\pi\nu_0 t + j\varphi(t)]$, where ν_0 is the center frequency and $\varphi(t)$ represents the intrinsic laser phase noise at time t. The frequency fluctuations $\Delta\nu(t)$ could be estimated statistically by the FNS $S_{\Delta\nu}(f)$.

The DSI system usually employs an unbalanced Mach-Zehnder interferometer (UMZI) where the laser output is split into two branches. One is modulated with a frequency of f_M [21], [22] and the other one passes through a fiber delay τ. The two branches are recombined and detected by a balanced photo-detector (BPD) before subsequently digitized. The acquired photocurrent can be

expressed as:

$$i(t) = \eta \left| \sqrt{\gamma} E(t-\tau) + e^{j2\pi f_M t} E(t) \right|^2 = 2\eta\sqrt{\gamma} E_0^2 \cos\left(2\pi f_M t + 2\pi \nu_0 \tau + \Delta\varphi_{t,\tau}\right) + DC \tag{1}$$

where η is the receiver sensitivity, γ is the power ratio between the interfering fields, $\Delta\varphi_{t,\tau} = \varphi(t) - \varphi(t-\tau)$ is the phase difference which could be estimated statistically by the beat note phase noise spectrum $S_{\Delta\varphi}(f)$, and DC is a direct-current part.

The ACF of the beat signal can be utilized to accumulate for the instantaneous phase over measurement time T. The normalized ACF [15] can be written as:

$$\Re_i(T) = \frac{1}{2\eta^2\gamma E_0^4} \langle i(t) i(t+T) \rangle = \cos(2\pi f_M T) \exp\left[-8 \int_{-\infty}^{+\infty} \frac{\sin^2(\pi T f) \sin^2(\pi \tau f)}{f^2} S_{\Delta\nu}(f) df \right] \tag{2}$$

Here we propose the theoretical description of the FIFT model for the first time. The ACF of DSI beat signal expressed in Eq. (2) could be converted with the identity $\cos(2\pi Tf) = 1 - 2\sin^2(\pi Tf)$, yielding:

$$\Re_i(T) = \cos(2\pi f_M T) \exp\left[-\sigma_{\Delta\varphi}^2(\tau) + \frac{1}{2} \int_{-\infty}^{+\infty} S_{\Delta\varphi}(f) \left(e^{j2\pi Tf} + e^{-j2\pi Tf} \right) df \right] \tag{3}$$

where $\sigma_{\Delta\varphi}^2(\tau) = \left\langle \Delta\varphi_{t,\tau}^2 \right\rangle$ is the variance of the beat note phase noise difference. According to the UMZI transform function $T(f) = 4\sin^2(\pi\tau f)/f^2$ [23], $S_{\Delta\varphi}(f)$ can be achieved by:

$$S_{\Delta\varphi}(f) = T(f) S_{\Delta\nu}(f) \tag{4}$$

Since $S_{\Delta\varphi}(f)$ is an even function, Eq. (3) could be further simplified into:

$$\Re_i(T) = \cos(2\pi f_M T) \exp\left[-\sigma_{\Delta\varphi}^2(\tau) + \Re_{\Delta\varphi}(T) \right] \tag{5}$$

where $\Re_{\Delta\varphi}(T) = \mathcal{F}^{-1}[S_{\Delta\varphi}(f)]$ is the ACF of the beat note phase noise difference and $\mathcal{F}^{-1}\{\cdot\}$ denotes inverse Fourier transform. By applying Fourier transform to Eq. (5), the double-sideband (DSB) power spectrum density (PSD) of the DSI signal can be written as:

$$S_i(f) = \frac{1}{2} \exp\left(-\sigma_{\Delta\varphi}^2\right) G(f \pm f_M) \tag{6}$$

where $G(f) = \mathcal{F}\{\exp[\Re_{\Delta\varphi}(T)]\}$ represents the phase noise distribution around the beat signal and $\mathcal{F}\{\cdot\}$ denotes Fourier transform. The single-sideband (SSB) PSD of the DSI signal can be expressed as:

$$S_i^1(f) = \exp\left(-\sigma_{\Delta\varphi}^2\right) G(f - f_M) \tag{7}$$

wherein the superscript 1 denotes the SSB nature of this PSD.

Through a pair of Fourier transform and inverse Fourier transform, such FIFT model directly connects the DSI spectrum with the actual laser FNS regardless of the FNS shape, permitting to evaluate the noise distribution of the DSI beat note induced by laser with arbitrary frequency noise characteristics. In addition, there is no extra limit on the delay time τ, implying the effectiveness in predicting the system performance in correlated, partially correlated, or uncorrelated cases.

2.2 Numerical Verification

To numerically verify the FIFT model, we compare it with conventional models. The comparison in DSI cases with different laser frequency noise including white noise (solid grey line), flicker noise (solid yellow line) and both white and flicker noise (solid blue line) is illustrated in Fig. 1.

The normalized ACF of DSI beat note with only white laser frequency noise is presented in Fig. 1(a). As described in [15], the conventional ACF consists of two separate sections: $|T| < \tau$ and $|T| \geq \tau$. It is worth noting that even though Eq. (5) is not in the segmentation form as the LLB model, the FIFT model could still successfully present the transition at the delay time τ, where the ACF envelope transforms from exponentially decaying into a constant amplitude. The ACF of the

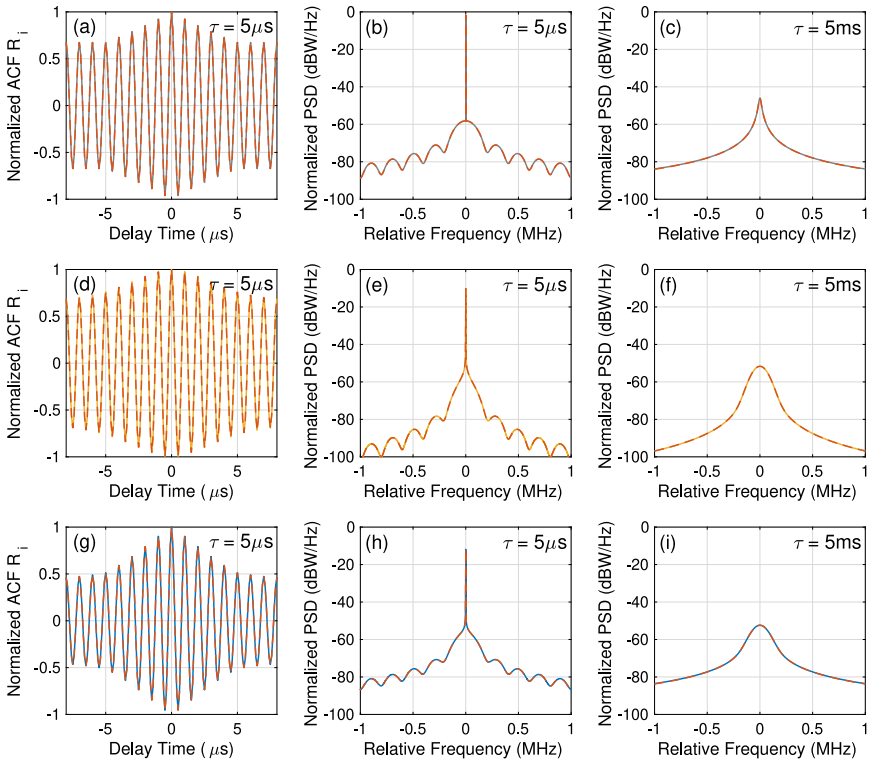

Fig. 1. Comparison of the ACF and PSD of DSI signal between the FIFT model (dashed red line) and the conventional models with white frequency noise (solid grey line), flicker frequency noise (solid yellow line), both white and flicker frequency noise (solid blue line) at 5 μs and 5 ms delay, respectively. (a)–(c) The ACF and DSI spectra with white frequency noise ($h_0 = 2 \times 10^3$ Hz^2/Hz). (d)–(f) The ACF and DSI spectra with flicker frequency noise ($k_1 = 1 \times 10^8$ Hz^3/Hz). (g)–(i) The ACF and DSI spectra with both two types of frequency noise ($h_0 = 2 \times 10^3$ Hz^2/Hz, $k_1 = 1 \times 10^8$ Hz^3/Hz).

flicker frequency noise is a product of the sinusoidal term and several power functions as indicated in [16]. As presented in Fig. 1(d), the envelope of the ACF is still decaying after the delay time and the FIFT model accurately describes the same evolution tendency. In the FFB model, the DSI ACF arising from both white and flicker frequency noise is the product of the ACF associated with each noise, respectively (see Fig. 1(g), solid blue line). Clearly, the FIFT model, although without the employment of the conventional multiplication method, is still valid in this case. Therefore, this confirms that the FIFT model is able to retrieve the ACF in all possible cases.

As illustrated in Fig. 1, DSI spectra at two different delays are investigated. These two cases, one is shorter and the other one is longer than coherence time, are chosen to represent two typical regimes of interference, coherent or incoherent. It verifies that, with various types of frequency noise, the FIFT model is capable to show how the noise distribution around the beat note evolves from short delay 5 μs (see Figs. 1(b), 1(e), and 1(h)) to long delay 5 ms (see Figs. 1(c), 1(f), and 1(i)), accordingly. The conventional models are, however, only able to handle certain cases with specific kinds of noise. In addition, the FIFT model also permits accurate prediction with different lineshapes including not only the Lorentzian lineshape but also the approximate Gaussian lineshape as illustrated in Figs. 1(c) and 1(f). When both white and flicker frequency noise is considered, in the FFB model, the DSI spectrum could be obtained through their convolution (see Figs. 1(h) and 1(i), solid blue line) as discussed above. This treatment is, nevertheless, complex and involves massive calculation. Such a kind of Voigt spectrum can also be directly and conveniently obtained using the FIFT model (see Fig. 1(i), dashed red line).

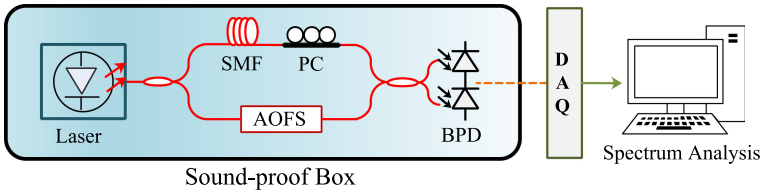

Fig. 2. Schematic of DSI system for experimental validation. SMF, single-mode fiber; PC, polarization controller; AOFS, acousto-optic frequency shifter; BPD, balanced photo-detector; and DAQ, data acquisition card.

Considering the fitting and convolution process, the computation complexity of the conventional methods is $\mathcal{O}(N^2)$. In comparison, the computation complexity ($\mathcal{O}(N\log N)$) of the FIFT model is much lower which represents computational convenience. To summarize, in contrast to the conventional models, if multiple types of frequency noise are considered simultaneously, the FIFT model could always offer an accurate and convenient estimate in a more compact and uniformed form without losing any details.

3. Experimental Setup

To verify the effectiveness and accuracy of the FIFT model, further experiments are conducted for DSI systems with different types of laser frequency noise. Practical demonstrations of the DSI system at different fiber delays are implemented to achieve the actual results of DSI spectra. The validation experiment schematic is presented in Fig. 2. The output light of the laser under test (LUT) is split into two branches by a polarization-maintaining coupler (PMC). One is modulated by an acousto-optic frequency shifter (AOFS) with a frequency of $f_M = 1$MHz to avoid the low-frequency noise of photo-detector which is under 200 kHz. The other one passes through a single-mode fiber of different delays. To prove the robustness of the model, experiments are carried out in different interferometric cases: correlated, partially correlated, or uncorrelated, using fiber delays that are within or beyond coherence length. A polarization controller (PC) is used to control the polarization. These two branches are recombined and detected by BPD before subsequently, digitized using a data acquisition card (DAQ). With the acquired photocurrent data, the actual DSI spectra can be calculated using the Welch method. A sound-proof box set onto a passive vibration isolation platform is utilized to reduce the potential environmental disturbances such as acoustic perturbations and mechanical vibrations. In this experiment, the thermal influence is negligible because the ambient temperature change is relatively slow and the detection time is quite short to be less than 1 s. The validation experiments are carried out inside the sound-proof box to ensure that laser frequency noise is the only noise source.

Different laser sources are respectively employed in the validation experiments including a single-mode fiber laser and a laser with irregular FNS. Besides, to prove the feasibility of the FIFT model, DSI experiments with laser employing a homemade optoelectronic phase-locked loop (OPLL) are conducted. The experimental setup of the OPLL is almost the same as the generation module in [23]. The aforementioned single-mode fiber laser is additionally stabilized to an all-fiber based UMZI. The error signal in proportion to the frequency fluctuation is fed back into the laser driver, forming a closed-loop control system that instantaneously suppresses the laser frequency noise. Polarization maintaining fiber-optic components are used within the loop to avoid polarization issues.

Before applying the FIFT model to estimate the DSI performance, the laser FNS is obtained in advance. In this paper, the laser FNS is previously measured by short delayed self-heterodyne (SDSH) method [24] as illustrated in Fig. 3. Then we substitute the FNS $S_{\Delta\nu}$ and corresponding delay τ into Eq. (5) and Eq. (7) to achieve the ACF and DSI spectra at arbitrary fiber delays. Comparing Figs. 3(a) and (c), with the employment of OPLL, the low-frequency frequency noise has been considerably reduced.

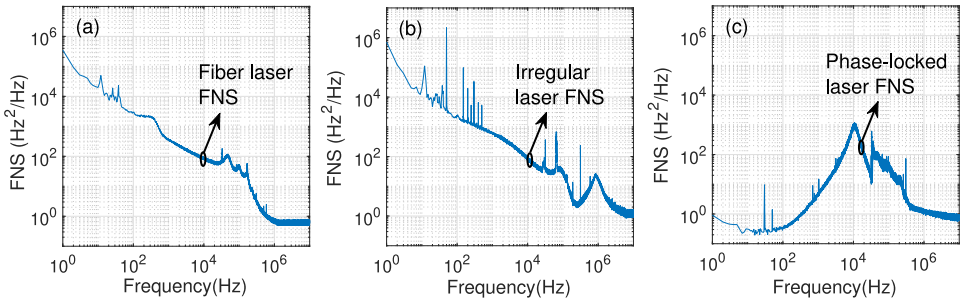

Fig. 3. Three different types of actual laser FNS. (a) Fiber laser FNS. (b) Irregular laser FNS. (c) Phase-locked laser FNS.

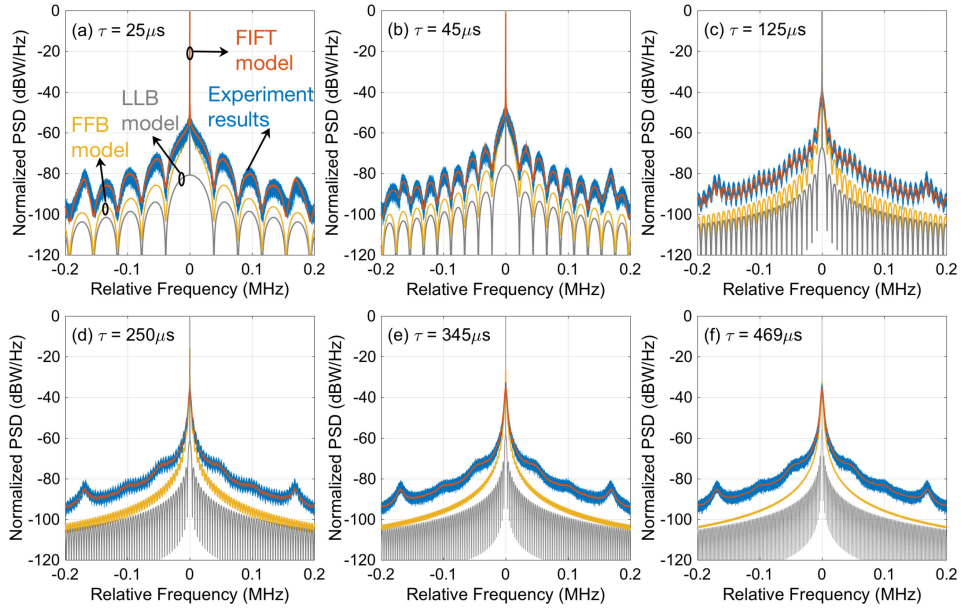

Fig. 4. Actual and estimated DSI spectra at different fiber delays. Blue line: experimental DSI spectra; red line: estimation results using the FIFT model; yellow line: estimation results via the FFB model; and grey line: estimation results by the LLB model.

The experiment results of DSI systems using different laser sources are compared with model estimation results respectively. In Section 4.1, comparative analysis between experiment results, estimation of the FIFT model, and the conventional models is presented. In Sections 4.2 and 4.3, using lasers with irregular FNS and OPLL, model validation with experimental data is carried out.

4. Experimental Validation

4.1 Model Comparison

In this section, a commercial single-mode fiber laser is employed to test and compare the conventional models and FIFT model. The laser FNS is illustrated in Fig. 3(a). The laser linewidth estimated by the power-area method (PAM) [25] is ∼3.51 kHz. DSI experiments employing the aforementioned laser at different delays from 5 to 95 km are carried out. In Fig. 4, the comparison between practically detected DSI spectra (see Fig. 4, blue line) at different fiber delays and estimates by different models are presented. In the following, the LLB model and FFB model are both applied to estimate the DSI performance.

TABLE 1
Estimation Goodness of Different Models

Model	Estimation goodness at various delays						
	25 μs	45 μs	125 μs	250 μs	345 μs	469 μs	Average
FIFT model	0.9867	0.9803	0.9705	0.9645	0.9622	0.966	0.9716
FFB model	0.9273	0.8057	0.6143	−1.571	0.5745	0.5419	0.3155
LLB model	0.85	0.5331	−11.122	−3621.2	−5116.6	−5558.2	−2384.3

Generally, if only white frequency noise is considered, the DSI spectrum can be calculated using the LLB model. According to Fig. 3(a), the white noise coefficient $h_0 = 0.315$ Hz^2/Hz is achieved. Laser linewidth contributed by purely white frequency noise can be calculated using FWHM $= 2\pi h_0$. The resulting DSI spectra estimates (see Fig. 4, grey line) are obviously different from the actual results probably because the low-frequency components are ignored in this model.

For the FFB model, the DSI spectra can be obtained with the extracted white noise coefficient $h_0 = 0.315$ Hz^2/Hz and 1/f noise coefficient $k_1 = 9.888 \times 10^4$ Hz^3/Hz, (see Fig. 4, yellow line). This estimation exhibits a lower noise level as many details cannot be analytically restored by this method. For example, in the actual FNS, anomalous spikes and uplifts around 30 kHz offset which do not have analytic solutions cannot be properly included in the fitting process.

In contrast to the conventional models, the laser FNS presented in Fig. 3(a) is directly employed in the FIFT model without fitting or any approximation. The estimation achieved by the FIFT model (see Fig. 4, red line) precisely tracks the tendency of the noise distribution with respect to different delay lengths in actual DSI experiments. Comparing the experiments and estimation results, the estimation goodness (EG) of different models in the form of R-square value is presented in Table 1. The value range of EG is from negative infinity to 1. At all the different delays, the FIFT model achieves EG of values closer to 1 than the conventional models, representing more accurate and precise estimates. The FIFT model offers AEG of 0.9716, indicating an obvious advantage over the FFB model (with AEG of 0.3155) and LLB model (with AEG of −2384.3). Compared with the actual detection, the evolution from the approximate sinc^2 function with dips at intervals of the reciprocal of the delay time to the approximate Voigt spectrum along with increased delays (from ∼25 to ∼469 μs) has been almost ideally restored. Even the bulges and fluctuations corresponding to the uplifts of the laser FNS around 0.05, 0.1, and 0.2 MHz, as well as the spikes and other artificial noise, are accurately reproduced in all the different states of interference. This experiment constitutes a solid confirmation of the accuracy of our model.

4.2 Free-Running Laser With Irregular FNS

Another commercial single-mode fiber laser with an irregular FNS (see Fig. 3(b)) is employed to testify our model. It can be observed that there are a lot of non-ignorable spikes and distortions around 65 kHz probably owing to the resonances in electrical driving circuity, gain peaks around natural frequencies, or other artificial oscillations. DSI demonstrations employing this laser are carried out at different fiber delays and the detected DSI spectra are illustrated in Fig. 5, blue line. The laser FNS shown in Fig. 3(b) is directly employed in the FIFT model to evaluate the DSI performance at corresponding delays as sketched in Fig. 5, red line. Such anomalous FNS properties are transferred into the humps at different interferometric conditions as anticipated via the FIFT model. Meanwhile, a similar evolution with respect to the ratio of the coherence time and the delay has been found accordingly, though due to the existence of those protrusions, the spectra hardly follow the common Lorentzian or Voigt lineshapes.

It is interesting that the spikes do not strictly follow the exponential decaying when the delay increases. This is due to the fact that at some certain delays, the spike almost coincides with the transmission null, namely the dips, in the UMZI transform function. For instance, in Fig. 5(e), the artificial spike around 313 kHz is strongly attenuated by the dip located at the integer multiple of

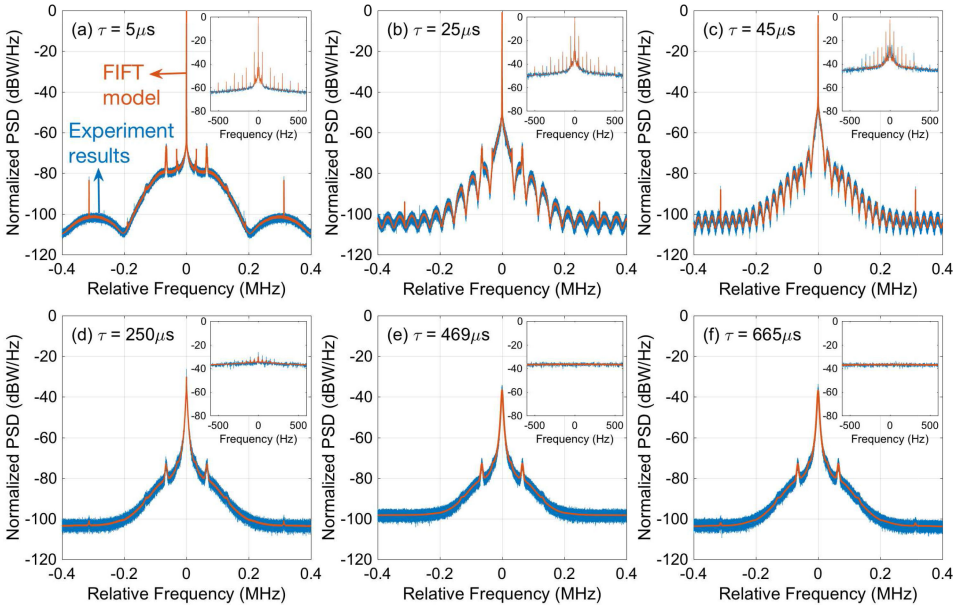

Fig. 5. Actual and estimated DSI spectra at different fiber delays. Blue line: detected DSI spectra; and red line: estimation results using the FIFT model.

the frequency interval of the reciprocal of the 469 μs delay. This also applies to the spikes and distortions around 65 kHz. As has been evidenced here, such kinds of irregular FNS behaviors and anomalous noise components that can be hardly handled by the conventional models can be transparently involved in the FIFT model losslessly.

4.3 Phase-Locked Laser

From an application point of view, to reduce the intrinsic laser frequency noise, one powerful technique is the OPLL, which allows for precise control of the laser frequency and phase and thereby, enhances the coherence. For a typical OPLL, relying on the feedback control with respect to references such as other lasers sources or optical etalons, the frequency, and phase distribution within a certain bandwidth follows that of the reference in closed-loop operation, suppressing the in-band fluctuations if a quieter reference is employed. Since OPLL introduces a strong modification of the FNS, clearly laser linewidth alone can no longer properly represent the coherence property of the laser. Moreover, the simple collection of multiple pre-defined types of noise including white and flicker frequency noise components with their corresponding coefficients are insufficient. It is thus quite emergent to validate the FIFT model in this circumstance.

With the presence of OPLL, the closed-loop FNS for the same laser used in Fig. 3(a), Section 4.1, is shown in Fig. 3(c). The PAM estimated closed-loop linewidth is $\sim$4.5 Hz. DSI experiments with the employment of the phase-locked laser are carried out at different fiber delays from 5 to 95 km. We compare the estimation results offered by the FIFT model (see Fig. 6, red line) with the detected DSI spectra (see Fig. 6, blue line). The estimation exhibits nearly every detail including the bulge around 10 kHz, the spikes around 30 kHz, and the uplift around 70 kHz. The bulge around 10 kHz is due to gain peaks around the natural frequency of the OPLL system transfer function. The FIFT model successfully presents that with fiber delay increases, the bulges do not move while the ripples caused by self-interference get closer. Comparing Fig. 4 and Fig. 6, the effect of the OPLL is observed: compression of laser linewidth, increasing of the signal peak power, and suppression of the in-band frequency noise. The closed-loop beat note spectrum still shows a distinct peak at the delay of 469 μs (see Fig. 6(f)) while the peak of the free-running beat note spectrum at the

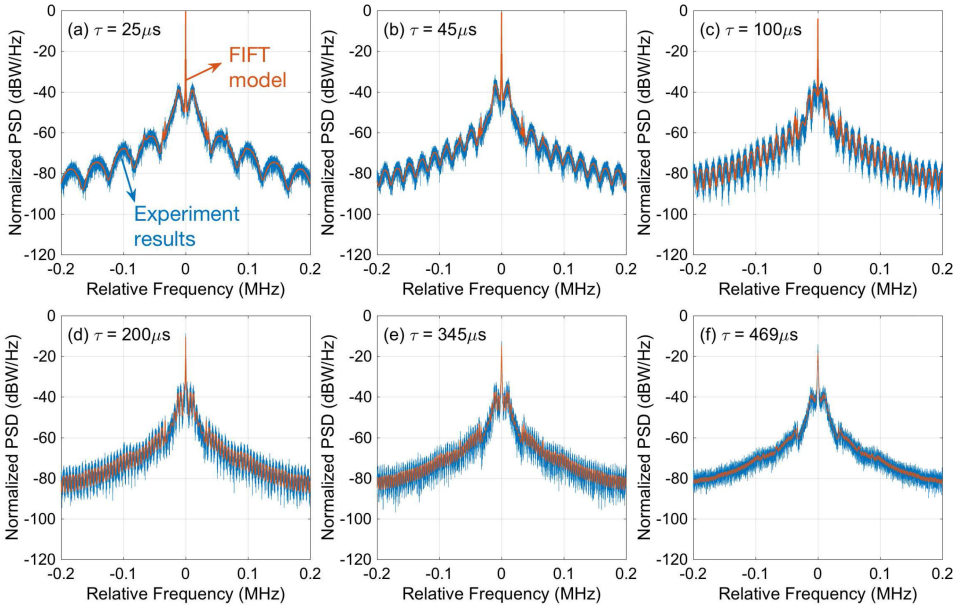

Fig. 6. Actual and estimated DSI spectra with the phase-locked laser at different fiber delays. Blue line: detected DSI spectra; and red line: estimation results using the FIFT model.

delay of 345 μs (see Fig. 4(e)) has been overwhelmed by the noise arising from the incoherent beating. The prominence of the beat note peak degrades as the delay increases. Nevertheless, because of the strong distortion in FNS, the evolution of the DSI spectra no longer follows that without the OPLL, but in a quite anomalous manner. This tendency has been closely tracked by the FIFT model as expected in comparison with the experiment results.

It proves that the FIFT model offers an effective approach in assessing the sophisticated spectra evolution with the presence of OPLL. Therefore, in the regime where conventional models fail, especially servo-induced anomalous frequency noise properties, it is really attractive that the FIFT model acts as a versatile approach with high accuracy, precision, efficiency, and robustness.

5. Application

In practical systems based on DSI structures, in order to analyze the noise performance and optimize the system, it is very important to distinguish the contributions from different noise sources, in particular, the contribution from the laser source, since the laser frequency noise is one fundamental limiting factor in the noise level of DSI system. Therefore, it is feasible to apply the proposed model to precisely quantify the contribution from the laser source, leading to the investigation and identification of the other potential noise sources in any DSI based systems.

As presented in Section 4, the experiments have proven that the performance limit caused by laser frequency noise can be evaluated precisely by the FIFT model. In the practical noisy operating environment, especially for large and complicated systems, it is difficult and costly to find appropriate isolation methods. Thus, considering practical system volume and complexity, comparative experiments in ideally stable environments or with appropriate isolation to identify the noise source are not feasible. To this end, without any experiments, the contribution of laser frequency noise can be conveniently restored by the FIFT model. In addition, the FIFT model applicable to arbitrary fiber delays avoids repeatable experiments. The assessment by the FIFT model (see Fig. 7, red line) which has been discussed in Section 4.1, successfully unveils the contribution.

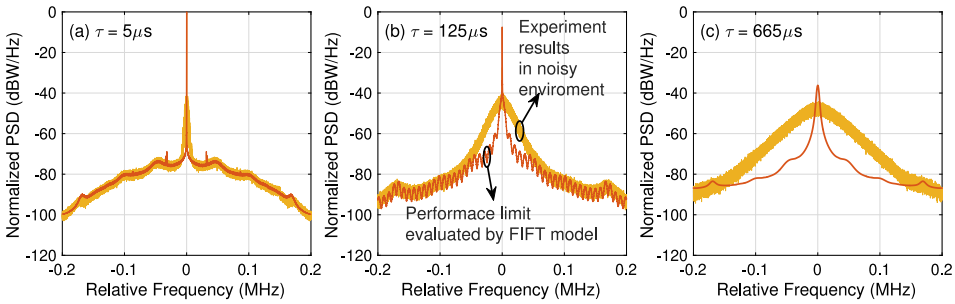

Fig. 7. The performance of DSI system with and without environment disturbances at different fiber delays. Yellow line: DSI spectra obtained in a noisy environment; and red line: laser intrinsic frequency noise causing performance limit evaluated by the FIFT model.

Experiments with similar configurations as stated in Section 3 and Section 4.1 are carried out when the fibers are placed on a normal table in a noisy lab environment without the sound-proof box. Compared with the performance limit assessed by the FIFT model (see Fig. 7(a), red line), the impact of the environment perturbations is mainly concentrated on the low-frequency region (see Fig. 7(a), yellow line) as dominated by the acoustic disturbances or vibrations below about 10 kHz. At all the delays, it is not surprising that the DSI system performance has been drastically deteriorated within this low-frequency bandwidth. In addition, the degradation becomes more serious at longer delays as the noise pedestal expands towards a higher frequency regime as illustrated in Figs. 7(b) and 7(c). It is thus clear that in this experiment, the noise performance is dominated by the environment perturbations, not by the intrinsic laser frequency noise. Improving the operation condition may achieve a better sensitivity to the DSI system.

Therefore, with the help of the proposed model, we are allowed to intuitively describe the contribution from laser itself to DSI systems, in any possible DSI cases and for any practical lasers with arbitrary FNS. This could be interesting for any DSI systems to distinguish the dominant noise source and for further performance optimization.

6. Conclusions

In this work, we present a compact and efficient approach, FIFT model, to precisely anticipate the performance limit caused by the laser frequency noise of any DSI system. Numerical and experimental comparisons prove the advantages of the FIFT model as follows:

1) The FIFT model is capable of evaluating the DSI system performance influenced by arbitrary laser frequency noise characteristics. While the conventional models are only applicable to specific types of frequency noise.
2) The FIFT model can be further applied to actual laser sources with irregular frequency noise properties or employing the OPLL while conventional methods cannot. Experimental comparison indicates that the estimations by the FIFT model agree well with the actual results in these situations where conventional models are invalid.
3) Real experiments confirm that the FIFT model provides AEG of 0.9716 which is much higher than conventional models with AEG lower than 0.3155, indicating greater accuracy and precision.
4) With a lower computation complexity of $\mathcal{O}(N\log N)$, the FIFT model is more computationally convenient than the conventional model ($\mathcal{O}(N^2)$). The processing flow of conventional methods including fitting and convolution is rather complicated than the FIFT model.

Moreover, the FIFT model can be utilized to assess the influence of environmental disturbances on practical DSI systems. With this model, it is quite feasible to distinguish the effects induced by the outside perturbations from that caused by the laser intrinsic frequency noise.

In conclusion, the FIFT model is attractive for laser interferometric system performance analysis and optimization in practical applications. It may also be of interest that this model can be further applied in other coherent system analyses such as coherent optical communication and optical sensing.

Acknowledgment

The authors wish to thank the anonymous reviewers for their valuable suggestions.

References

[1] H. Guan *et al.*, "Widely-tunable, narrow-linewidth iii-v/silicon hybrid external-cavity laser for coherent communication," *Opt. Express*, vol. 26, no. 7, pp. 7920–7933, 2018.
[2] K. Kikuchi, "Fundamentals of coherent optical fiber communications," *J. Lightw. Technol.*, vol. 34, no. 1, pp. 157–179, Jan. 2015.
[3] E. Ip, A. P. T. Lau, D. J. Barros, and J. M. Kahn, "Coherent detection in optical fiber systems," *Opt. Express*, vol. 16, no. 2, pp. 753–791, 2008.
[4] H.-H. Lu, G.-L. Chen, Y.-W. Chuang, C.-C. Tsai, and C.-P. Chuang, "Improvement of radio-on-multimode fiber systems based on light injection and optoelectronic feedback techniques," *Opt. Commun.*, vol. 266, no. 2, pp. 495–499, 2006.
[5] K. Kikuchi, "Characterization of semiconductor-laser phase noise and estimation of bit-error rate performance with low-speed offline digital coherent receivers," *Opt. Express*, vol. 20, no. 5, pp. 5291–5302, 2012.
[6] S. Dou *et al.*, "Distributed acoustic sensing for seismic monitoring of the near surface: A traffic-noise interferometry case study," *Scientific Rep.*, vol. 7, no. 1, pp. 1–12, 2017.
[7] K. Xu, Y. Chen, T. A. Okhai, and L. W. Snyman, "Micro optical sensors based on avalanching silicon light-emitting devices monolithically integrated on chips," *Opt. Mater. Exp.*, vol. 9, no. 10, pp. 3985–3997, 2019.
[8] A. Peigné *et al.*, "Adaptive interferometry for high-sensitivity optical fiber sensing," *J. Lightw. Technol.*, vol. 34, no. 19, pp. 4603–4609, Oct. 2016.
[9] T. DiLazaro and G. Nehmetallah, "Large-volume, low-cost, high-precision fmcw tomography using stitched dfbs," *Opt. Express*, vol. 26, no. 3, pp. 2891–2904, 2018.
[10] J.-P. von der Weid, R. Passy, and N. Gisin, "Mid-range coherent optical frequency domain reflectometry with a dfb laser diode coupled to an external cavity," *J. Lightw. Technol.*, vol. 13, no. 5, pp. 954–960, May 1995.
[11] J.-P. Von Der Weid, R. Passy, G. Mussi, and N. Gisin, "On the characterization of optical fiber network components with optical frequency domain reflectometry," *J. Lightw. Technol.*, vol. 15, no. 7, pp. 1131–1141, Jul. 1997.
[12] D. Pan, C. Ke, S. Fu, Y. Liu, D. Liu, and A. E. Willner, "All-optical spectral linewidth reduction of lasers for coherent optical communication," *Opt. Lett.*, vol. 38, no. 24, pp. 5220–5223, 2013.
[13] T. DiLazaro and G. Nehmetallah, "Phase-noise model for actively linearized frequency-modulated continuous-wave ladar," *Appl. opt.*, vol. 57, no. 21, pp. 6260–6268, 2018.
[14] P. Gallion and G. Debarge, "Quantum phase noise and field correlation in single frequency semiconductor laser systems," *IEEE J. Quantum Electron.*, vol. 20, no. 4, pp. 343–349, Apr. 1984.
[15] P. Gallion, F. Mendieta, and R. Leconte, "Single-frequency laser phase-noise limitation in single-mode optical-fiber coherent-detection systems with correlated fields," *Josa*, vol. 72, no. 9, pp. 1167–1170, 1982.
[16] L. B. Mercer, "1/f frequency noise effects on self-heterodyne linewidth measurements," *J. Lightw. Technol.*, vol. 9, no. 4, pp. 485–493, Apr. 1991.
[17] T. N. Huynh, L. Nguyen, and L. P. Barry, "Phase noise characterization of sgdbr lasers using phase modulation detection method with delayed self-heterodyne measurements," *J. Lightw. Technol.*, vol. 31, no. 8, pp. 1300–1308, Apr. 2013.
[18] M. Fleyer, J. P. Cahill, M. Horowitz, C. R. Menyuk, and O. Okusaga, "Comprehensive model for studying noise induced by self-homodyne detection of backward rayleigh scattering in optical fibers," *Opt. Express*, vol. 23, no. 20, pp. 25 635–25 652, 2015.
[19] W. Ma *et al.*, "Laser frequency noise characterization by self-heterodyne with both long and short delay," *Appl. Opt.*, vol. 58, no. 13, pp. 3555–3563, 2019.
[20] H. Tsuchida, "Limitation and improvement in the performance of recirculating delayed self-heterodyne method for high-resolution laser lineshape measurement," *Opt. Express*, vol. 20, no. 11, pp. 11 679–11 687, 2012.
[21] A. B. Greytak, C. J. Barrelet, Y. Li, and C. M. Lieber, "Semiconductor nanowire laser and nanowire waveguide electro-optic modulators," *Appl. phys. lett.*, vol. 87, no. 15, 2005, Art. no. 151103.
[22] K. Xu, "Silicon mos optoelectronic micro-nano structure based on reverse-biased pn junction," *Physica Status Solidi (a)*, vol. 216, no. 7, 2019, Art. no. 1800868.
[23] W. Xie *et al.*, "Fourier transform-limited optical frequency-modulated continuous-wave interferometry over several tens of laser coherence lengths," *Opt. Lett.*, vol. 41, no. 13, pp. 2962–2965, 2016.
[24] Q. Zhou, J. Qin, W. Xie, Y. Tong, Z. Liu, Y. Dong, and W. Hu, "Dynamic frequency-noise spectrum measurement for a frequency-swept dfb laser with short-delayed self-heterodyne method," *Opt. Express*, vol. 23, no. 22, pp. 29 245–29 257, 2015.
[25] Q. Zhou, J. Qin, W. Xie, Y. Tong, Z. Liu, Y. Dong, and W. Hu, "Power-area method to precisely estimate laser linewidth from its frequency-noise spectrum," *Appl. Opt.*, vol. 54, no. 28, pp. 8282–8289, 2015.